











Neutral point current is given by

$$i_0 = -i_1 + i_2 \quad (11)$$

$$i_0 = -C \frac{d(V_{c1} - V_{c2})}{dt} \quad (12)$$

The equation yields

$$V_{c1} - V_{c2} = -\frac{1}{C} \int i_0 dt + \text{constant} \quad (13)$$

This signifies that a DC component in the neutral current  $i_0$ , can be utilised to compensate the voltage dc link capacitor voltages of the converter.

### B. Auxiliary Circuit

As shown in the Figure.4 dc link capacitors  $C_1$  and  $C_2$  are connected to an auxiliary capacitor  $C_a$  through four switches. A series resistance  $r$  is connected with auxiliary capacitor  $C_a$  to limit the amplitude of the charging current for practical consideration. Whenever there is voltage difference between  $C_1$  and  $C_2$  there will be always charging and discharging current between one of the dc link capacitors ( $C_1$  or  $C_2$ ) and auxiliary capacitor  $C_a$ . To explain the balancing phenomena the whole operation is divided in to four cases.

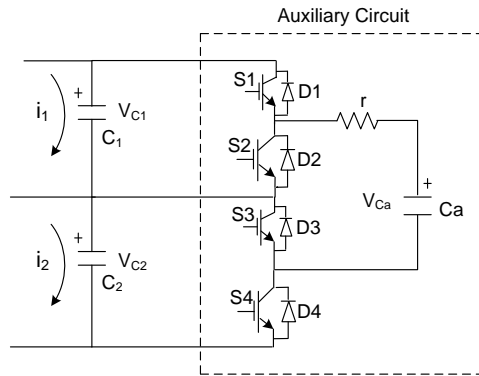


Figure.4 Auxiliary circuit for dc link capacitor voltage balancing

*Case 1: When  $V_{c1} > V_{ca}$*

In this condition, switch S1, S3 are turned on and switch S2, S4 are turned off. The charging current  $i_{ca}$  pumps from  $C_1$  to  $C_a$  through S1,  $r$  and D3 as highlighted in Figure. 5a.

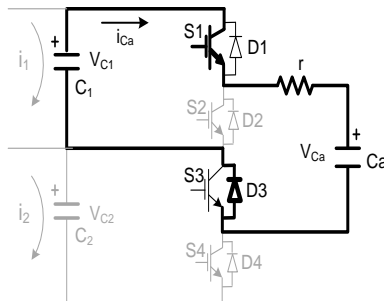


Figure 5a. Current flows from  $C_1$  to  $C_a$

*Case 2: When  $V_{c1} < V_{ca}$*

When voltage across auxiliary capacitor ( $V_{ca}$ ) is more than dc link capacitor  $V_{c1}$ , the switching action will remain the same i.e. S1, S3 are on and charging current  $i_{ca}$  comes from  $C_a$  through  $r$ , D1,  $C_1$  and S3 as highlighted in Figure 5b.

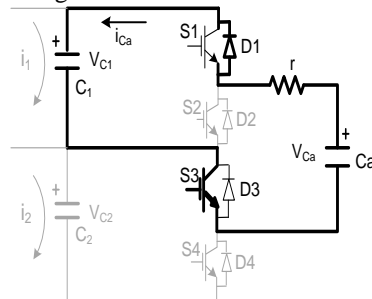


Figure 5b. Current flows from  $C_a$  to  $C_1$

*Case 3: When  $V_{c2} < V_{ca}$*

Under this condition, the switch S1, S3 are turned off and S2, S4 are now turned on. The charging current  $i_{ca}$  comes from  $C_a$  to  $C_2$  through  $r$ , S2, D4 as highlighted in Figure 5c.

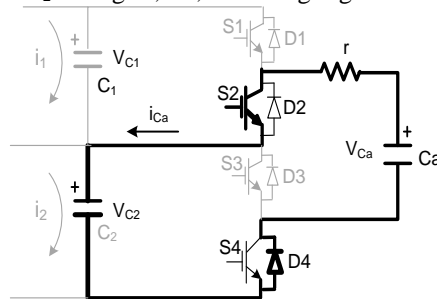


Figure. 5c Current flows from  $C_a$  to  $C_2$

*Case 4: When  $V_{c2} > V_{ca}$*

In this condition, switching action will again remain the same and the charging current  $i_{ca}$  pumps from  $C_2$  to  $C_a$  through D2,  $r$  and S4 as highlighted in Figure. 5d.

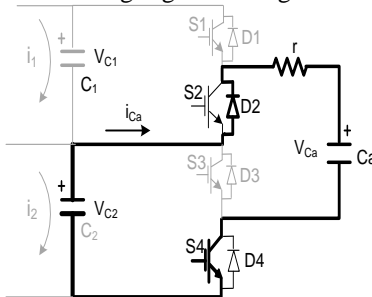


Figure 5d. Current flows from  $C_2$  to  $C_a$

The equivalent circuit for the Figure.4 is drawn and shown in the Figure.6. For the analysis purpose the equivalent circuit is drawn for *Case 1* and *Case 2* and same analysis is applicable for *Case 3* and *Case 4*.

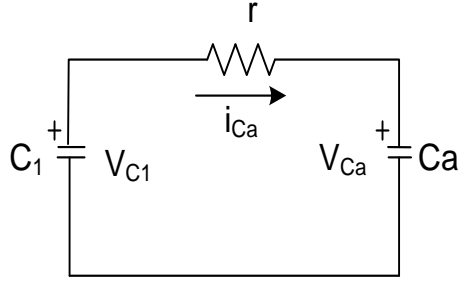


Figure 6. Equivalent circuit

If  $C_1$  and  $C_a$  are equal then the total capacitance of capacitors in series is equal to  $C/2$ . The voltage and the charging current in the simple RC circuit will be given below for the time period of  $t_0$  to  $t_1$ .

$$V(t) = V(t_0) - \frac{2}{C} \int_{t_0}^{t_1} i_{c1}(t) dt \quad (14)$$

$$i_{c1}(t) = \frac{V(t_a)}{r} e^{-\frac{2t}{rc}} \quad (15)$$

As explained earlier the balancing concept is based on ping pong operation and one ping pong operation is divided in to two time steps. Step 1 starts from time  $t_0$  and finish at  $t_1$  corresponding to *Case 1* & *2* of earlier section whereas time period for step 2 is  $t_1$ - $t_2$  corresponding to *Case 3* & *4* of earlier section. Then, the voltages across the  $C_1$ ,  $C_2$  and  $C_a$  can be expressed as,

$$v_{c1}(t) = \begin{cases} v_{c1}(t_0) - \frac{1}{C} \int_{t_0}^{t_1} i_{ca1}(t) dt, & t_0 \leq t \leq t_1 \\ v_{c1}(t_0), & t_1 \leq t \leq t_2 \end{cases} \quad (16)$$

$$v_{c2}(t) = \begin{cases} v_{c2}(t_0), & t_0 \leq t \leq t_1 \\ v_{c2}(t_1) - \frac{1}{C} \int_{t_1}^{t_2} i_{ca1}(t) dt, & t_1 \leq t \leq t_2 \end{cases} \quad (17)$$

$$v_{ca1}(t) = \begin{cases} v_{c1}(t_0) + \frac{1}{C} \int_{t_0}^{t_1} i_{ca1}(t) dt, & t_0 \leq t \leq t_1 \\ v_{c1}(t_1) - \frac{1}{C} \int_{t_1}^{t_2} i_{ca1}(t) dt, & t_1 \leq t \leq t_2 \end{cases} \quad (18)$$

Where the balancing current  $i_{ca}$  is

$$i_{c1}(t) = \begin{cases} \frac{v_{c1}(t_0) - v_{ca1}(t_0)}{r} e^{-\frac{2t}{rc}} & t_0 \leq t \leq t_1 \\ \frac{v_{c2}(t_1) - v_{ca1}(t_1)}{r} e^{-\frac{2(t-t_1)}{rc}} & t_1 \leq t \leq t_2 \end{cases} \quad (19)$$

According to (16-19), the voltage difference between  $C_1$  &  $C_2$  will decrease after a number of ping-pong operations.

Figure 7 shows the control scheme for the auxiliary circuit. This control scheme is generating PWM pulses for auxiliary circuit switches by comparing a signal of constant magnitude with triangular carrier wave such that S2 & S4 are the complimentary of S1 & S3 respectively for carrying out ping-pong operation.



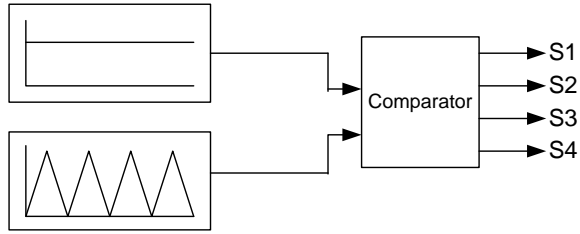


Figure 7. Control Scheme for auxiliary circuit.

#### 4. Result and Discussion

In this section, simulation results are presented and verified experimentally by developing laboratory prototype of neutral point clamped (NPC) active front end (AFE) 3-level converter.

##### A. Simulation Results

Simulation results are given for evaluating the performance of the neutral point clamped (NPC) active front end (AFE) 3-level converter using UPC. The simulation is carried out with and without NPP regulator in the UPC under balanced and unbalanced load conditions. The block diagram of simulation model is shown in Figure. 8 and simulation parameters are given in Table 2. The optimized controller parameters are given in Table 3.

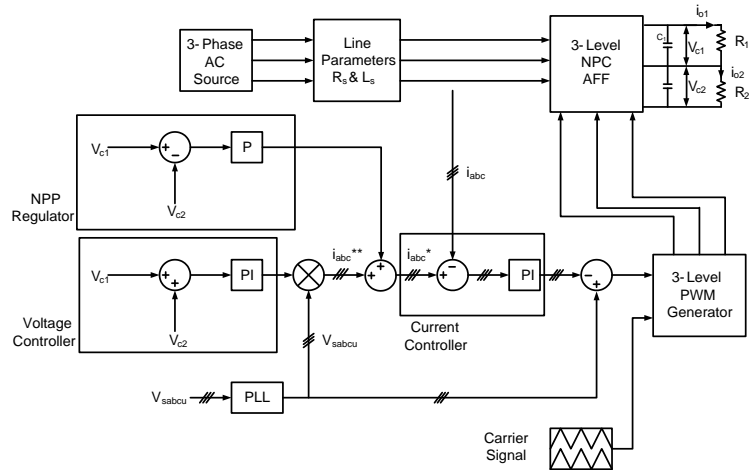


Figure. 8 Block diagram of neutral point clamped active front end 3-level converter with UPC

Table 2. Simulation Parameters for NPC AFE 3-Level Converter with UPC

Line Voltage (RMS)	$V_{LL}$	50 V
Boost Inductor	$L_s$	7.73mH
AC Link Resistance	$R$	0.1 $\Omega$
DC Link Voltage	$V_{dc}$	80 V
DC Link Capacitance	$C_1/ C_2$	2200 $\mu$ F
Load Resistance	$R_1 \parallel R_1'$	15 $\Omega \parallel$ 15 $\Omega$
	$R_2 \parallel R_2'$	15 $\Omega \parallel$ 15 $\Omega$
Carrier Frequency	$f_c$	2050 Hz

Table 3. Selected UPC Parameters for NPC AFE 3-Level Converter

Current Controller Parameters	
Proportional Gain ( $K_{cp}$ )	0.5
Integral Gain ( $K_{ci}$ )	10
Voltage Controller Parameters	
Proportional Gain ( $K_{vp}$ )	2
Integral Gain ( $K_{vi}$ )	25
NPP Regulator Parameters	
Proportional Gain ( $K_{np}$ )	2

### A.1 Performance of NPC AFE with UPC

Phase voltage of phase ‘a’, line current of phase ‘a’, dc link capacitor voltages ( $V_{c1}$  and  $V_{c2}$ ) and load current ( $i_o$ ) under steady state condition is shown in Figure. 9. This shows the stable operation of neutral point clamped active front end 3-level converter with unity power factor controller under steady state condition, which is essentially required for medium voltage, high power applications.

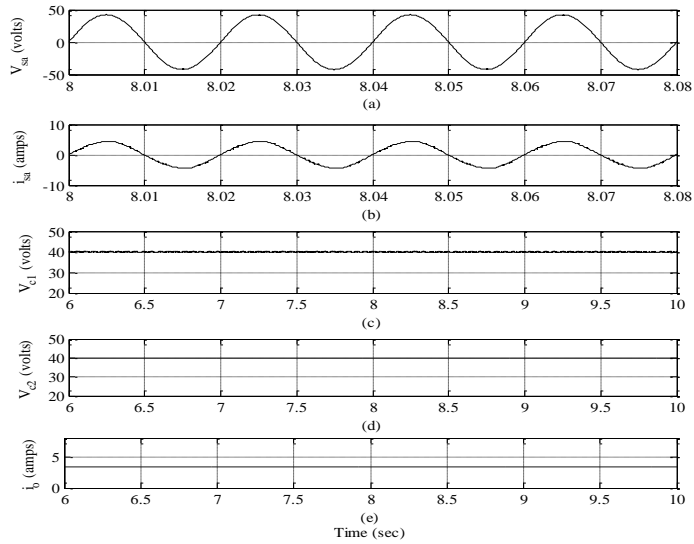


Figure 9. Phase voltage ( $V_{sa}$ ), Line current ( $i_{sa}$ ), dc link capacitor voltages ( $V_{c1}$  and  $V_{c2}$ ) and load current ( $i_o$ ) of NPC AFE 3-level converter under steady state condition

The dynamic performance of NPC AFE AC-DC converter is also evaluated with sudden load change as shown in Figure. 10 & Figure. 11. It is observed that the dc link capacitor voltages ( $V_{c1}$  and  $V_{c2}$ ) settled down to its desired value within 10 cycles, the supply

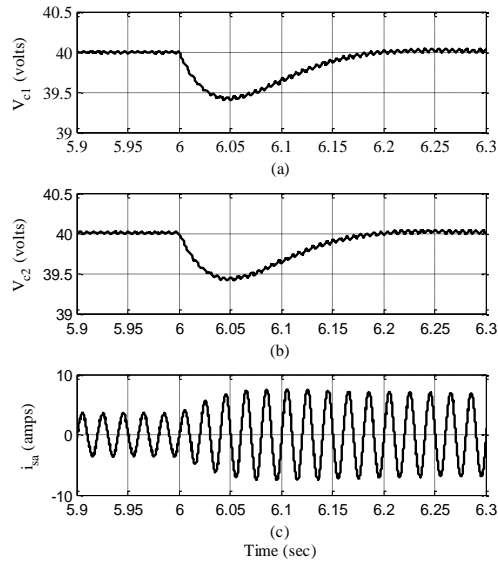


Figure 10. DC link Capacitor Voltages ( $V_{c1}$  and  $V_{c2}$ ), DC link Capacitor Voltage ( $V_{c1}$ ) and Source current ( $i_{sa}$ ) for increase in load at  $t = 5$  sec

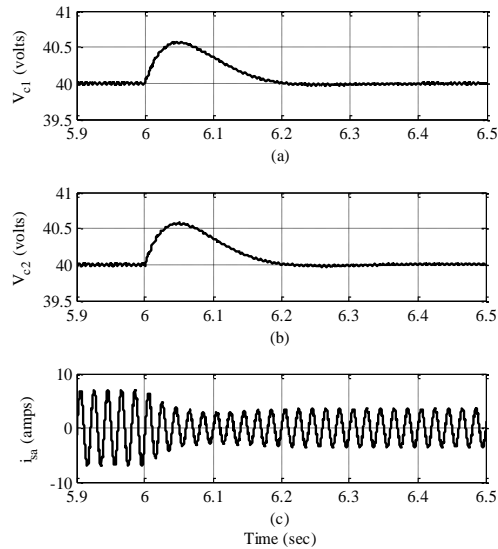


Figure 11. DC link Capacitor Voltages ( $V_{c1}$  and  $V_{c2}$ ), DC link Capacitor Voltage ( $V_{c1}$ ) and Source current ( $i_{sa}$ ) for decrease in load at  $t = 10$  sec

### A.2. Neutral Point Potential (NPP) Control Using NPP Regulator

The neutral point potential is basically difference between two dc link capacitor voltages. Ideally NPP should be zero i.e. balanced dc link capacitor voltages under transient and steady state conditions. In this study, simulation is carried out with and without NPP regulator in UPC under balanced and unbalanced load condition. The level of unbalance is measured by a factor defined as depth of unbalance  $\sigma$  as [27]

$$\sigma = \frac{R_1 - R_2}{R_1 + R_2} \times 100 \quad (20)$$

Where  $R_1$  load resistance is across dc link capacitor  $C_1$  and  $R_2$  is load resistance across dc link capacitor  $C_2$ .

The study is carried out for different depth of unbalance ( $\sigma$ ) to observe its effect on the performance of NPP regulator in UPC. The system parameters for the simulation are same given in Table 2. The details of loading parameters are given in Table 4

Table 4. Load Parameters

Resistance ( $R_1$ ) ( $\Omega$ )	Resistance ( $R_2$ ) ( $\Omega$ )	% Depth of unbalanced load ( $\sigma$ )
15	15	0
15	10	20
15	7.5	33.33

Figure 12 shows the NPP variation with and without NPP regulator. It clearly shows that there are variations in average of NPP under balanced load ( $\sigma = 0\%$ ). Even though the variation is not large, but it is significant for high voltage and high power applications. When NPP regulator is included in the UPC, the NPP variations got suppressed and NPP become almost zero as shown in the Figure. 12. Figure. 13 and Figure. 14 shows the variations of NPP with and without NPP regulator in UPC for  $\sigma = 20\%$  and  $\sigma = 33.33\%$  respectively. These Figure shows that the variations of NPP increases with depth of unbalance. The NPP regulator in UPC is capable to control the NPP variations as shown in Figure. 13 and Figure. 14.

Figure. 15 shows the dc link capacitor voltages ( $V_{c1}$  &  $V_{c2}$ ) before and after the NPP regulator included in the UPC. It also confirms the balancing of dc link capacitor voltages using NPP regulator in UPC.

Table 5 shows that, the NPP regulator in UPC removes the 2<sup>nd</sup> harmonic from supply line current whereas the dc off-set appears in the supply line current as depth of unbalance increase. The undesirable dc off-set in supply current will saturate the transformer on the utility side and must be removed from the supply current. Therefore, the NPP regulator in the UPC controls the variations in NPP under balanced load whereas for different depth of unbalance the NPP regulator able to control NPP variations at the cost of dc off-set in supply line current.

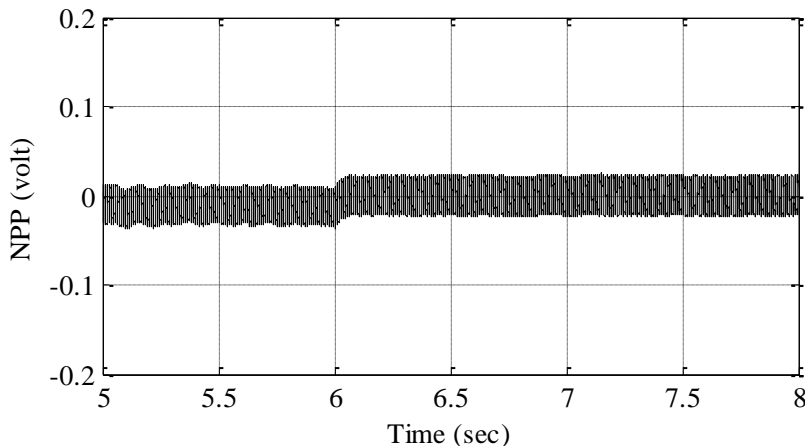


Figure 12. NPP before and after NPP regulator is included in UPC at  $t = 6$  sec for  $\sigma = 0\%$

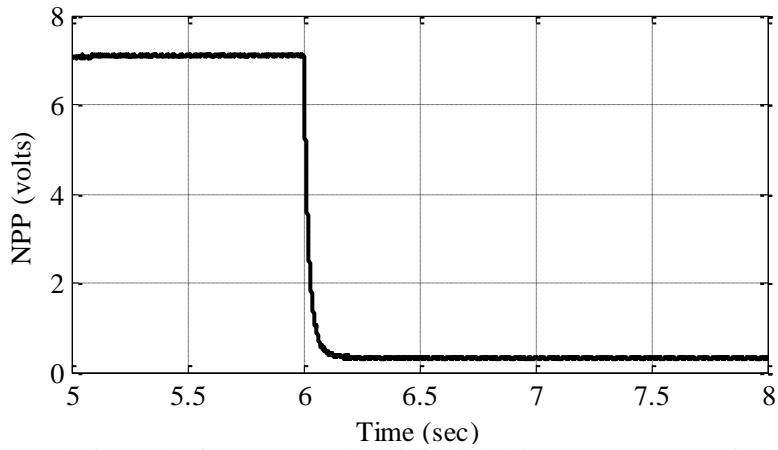


Figure 13. NPP before and after NPP regulator is included in UPC at  $t = 6$  sec for  $\sigma = 20\%$

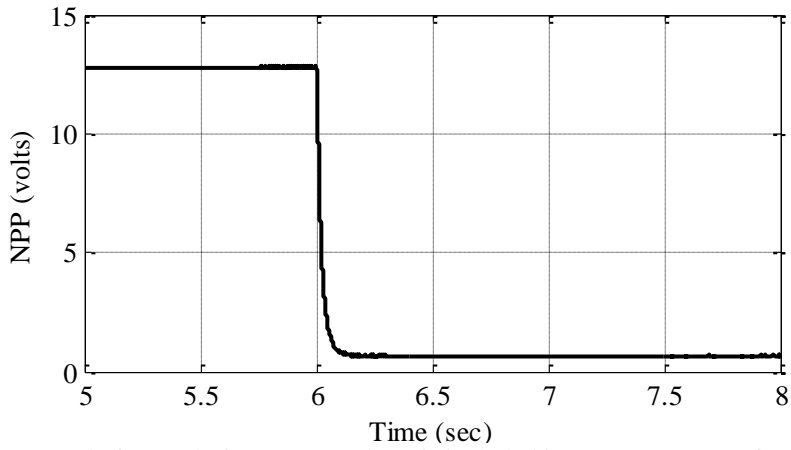


Figure 14. NPP before and after NPP regulator is included in UPC at  $t = 6$  sec for  $\sigma = 33.33\%$

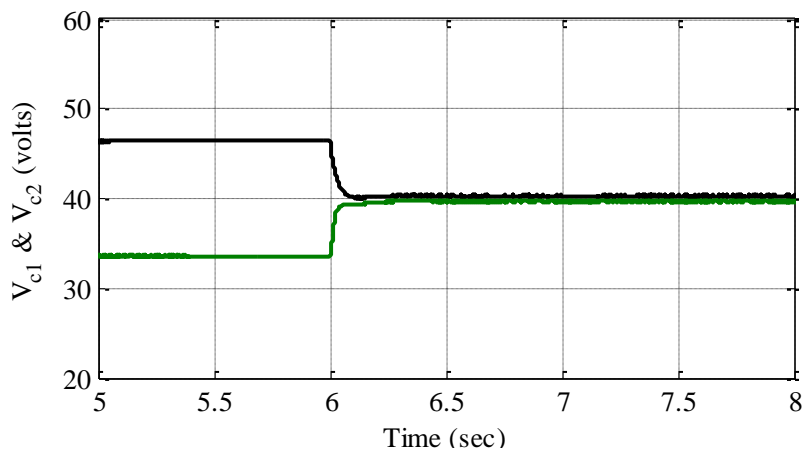


Figure 15. DC link capacitor voltages ( $V_{c1}$  &  $V_{c2}$ ) before and after NPP regulator is included in UPC at  $t = 6$  sec for  $\sigma = 33.33\%$

Table 5. Variation of DC offset & 2<sup>nd</sup> Harmonic with depth of unbalance ( $\sigma$ ) in Supply Line Current of Phase a ( $i_{sa}$ ) with and without NPP Regulator in UPC

Depth of Unbalance ( $\sigma$ )	DC Off-set and 2 <sup>nd</sup> Harmonic in Supply Line Current of Phase a ( $i_{sa}$ )			
	Without NPP Regulator		With NPP Regulator (%)	
	DC Off-set (%)	2 <sup>nd</sup> Harmonic (%)	DC Off-set (%)	2 <sup>nd</sup> Harmonic (%)
0%	0	0	0	0
20%	0	10	15%	0
33.33%	0	17	25%	0

### A.3. Neutral Point Potential (NPP) Control Using Auxiliary Circuit

A simulation has been carried out for AC-DC multilevel converter with an auxiliary circuit for  $\sigma = 33.33\%$ . As shown in Figure.16 the average NPP is become almost zero when auxiliary circuit is included at  $t = 6$  sec. Figure.17 shows the voltage across the dc link capacitors ( $V_{c1}$  &  $V_{c2}$ ) before and after the auxiliary circuit is included in system. The simulation confirms that the adopted voltage balancing scheme using auxiliary circuit is maintaining almost equal voltage across the dc link capacitors. Table 6 also shows that the auxiliary circuit balances dc link voltage without dc offset in the input line current for different depth of unbalance load.

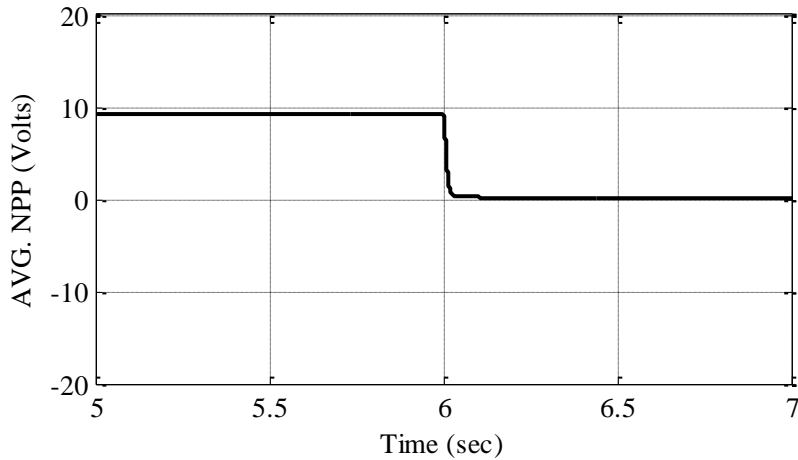


Figure 16. Average NPP when auxiliary circuit is included at  $t = 6$  sec for  $\sigma = 33.33\%$

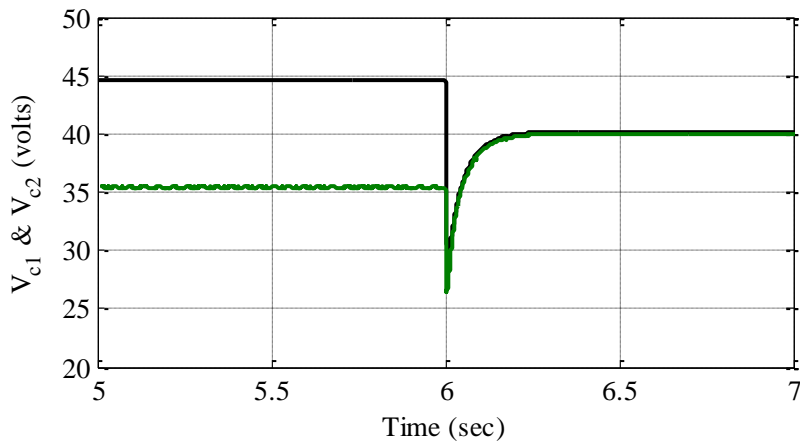


Figure.17 DC link voltages ( $V_{c1}$  &  $V_{c2}$ ) when auxiliary circuit is included at  $t = 6$  sec for  $\sigma = 33.33\%$

Table 6. Variation of DC offset & 2<sup>nd</sup> Harmonic with depth of unbalance ( $\sigma$ ) in Supply Line Current of Phase a ( $i_{sa}$ ) with Auxiliary Circuit

Depth of Unbalance ( $\sigma$ )	DC Off-set and 2 <sup>nd</sup> Harmonic in Supply Line Current of Phase a ( $i_{sa}$ ) with Auxiliary Circuit	
	DC Off-set (%)	2 <sup>nd</sup> Harmonic (%)
0%	0	0
20%	0	0
33.33%	0	0

### B. Experimental Results

The performance of NPC AFE 3-level converter is verified experimentally on developed low power prototype in laboratory. The experimental parameters for NPC AFE 3-level converter are given in Table 7. The prototype of AC-DC converter includes twelve STGW30N120KD, 1200 volts, 30 amps IGBTs and six fast recovery diodes (16FM120) with two dc link capacitors of 2200mF, 600 V each at input side. The control algorithm is implemented through dSPACE real time interface DS1103. The DS1103 real time hardware implementation board is based upon Texas Instruments TMS320F240, 16 bit fixed point digital signal processor, 250 MHz CPU, 20 MHz clock frequency.

Table 7. Experimental Parameters

Line Voltage (RMS)	$V_{LL}$	50 V
Source Inductor	$L_s$	7.73mH
AC Link Resistance	R	0.4 $\Omega$
DC Link Parameters		
DC Link Voltage	$V_{dc}$	80 V
DC Link Capacitors	$C_1$ and $C_2$	2200 $\mu$ F
Load Parameters		
Load Resistance	( $R_1$ and $R_2$ )	15 $\Omega$
Carrier Frequency	$f_c$	2050 Hz

#### B.1. Performance of NPC AFE with UPC

The line voltage ( $V_{ab}$ ) at supply end, supply phase voltage ( $V_{sa}$ ) and line current ( $i_{sa}$ ) are shown in Figure. 18, which clearly shows unity power factor operation of the converter. The harmonic profile of the line voltage ( $V_{ab}$ ) at supply end and line current ( $i_{sa}$ ) are shown in Figure. 19 (a) and Figure. 19 (b) respectively. The line current ( $i_{sa}$ ) drawn by NPC AFE 3-level converter is having only 2.4% of THD, which is well below the limit imposed by standard IEEE 519.

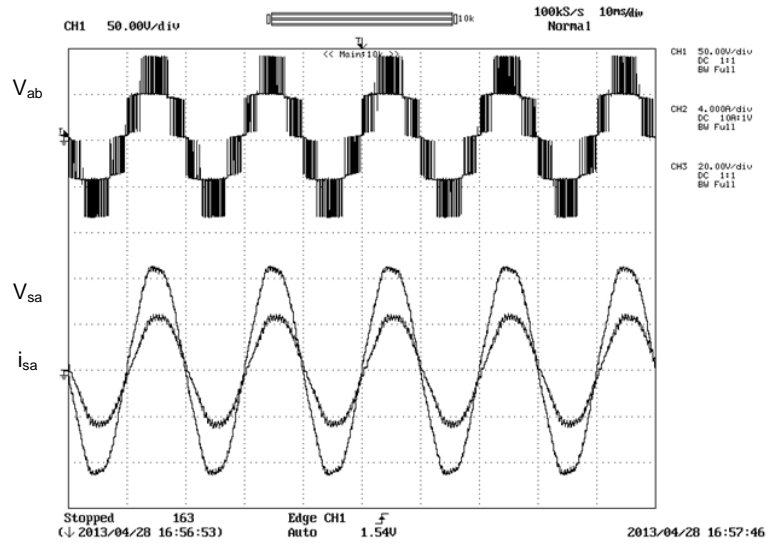
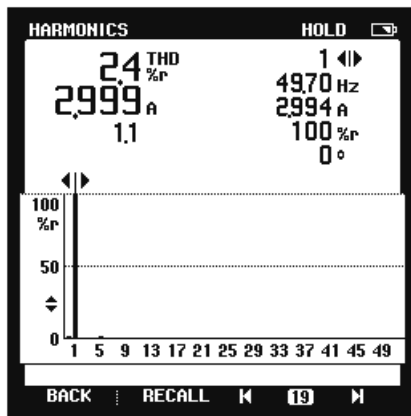
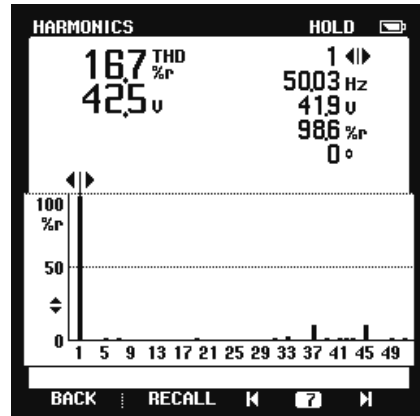


Figure 18. Converter line voltage ( $V_{ab}$ ), phase voltage ( $V_{sa}$ ) and line current ( $i_{sa}$ ) of NPC AFE 3-level converter

X - axis: Time – 10ms/div, Y axis:  $V_{ab}$  – 50 V/div,  $V_{sa}$  – 20V/div and  $i_{sa}$  – 4A/div



(a)



(b)

Figure.19 Harmonic spectrum of (a) Line current ( $i_{sa}$ ) and (b) converter line voltage.

The performance of NPC AFE 3-level converter under steady state condition has been verified experimentally. The phase voltage ( $V_{an}$ ) at supply end is shown in Figure. 20 under steady state condition which confirms one of the important features of multilevel converter having half of the dc link voltage subjected across the devices. The voltage across the dc link capacitors ( $V_{c1}$  and  $V_{c2}$ ) are shown in Figure. 21 under steady state condition. This shows stable operation of converter under steady state condition.



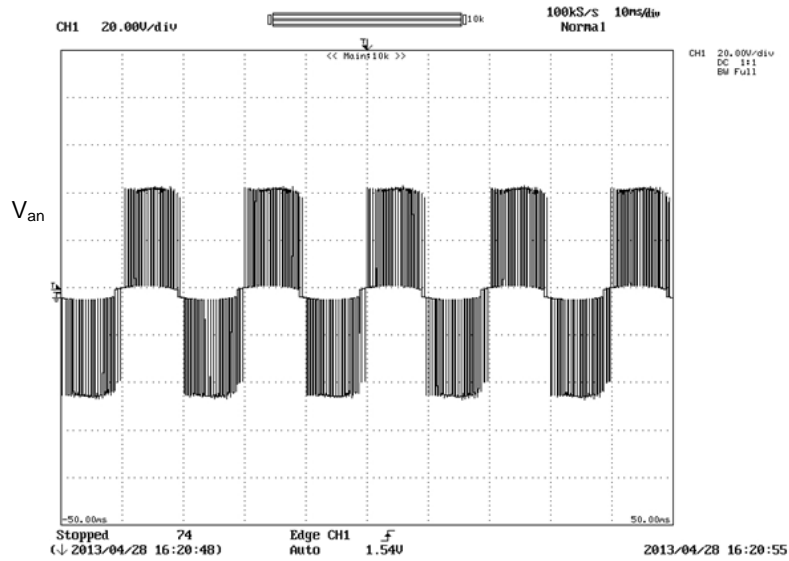


Figure 20. Phase voltage ( $V_{an}$ ) at supply end of NPC AFE 3-level converter under steady state condition

X - axis: Time –10ms/div, Y - axis:  $V_{an}$  - 20 V/div

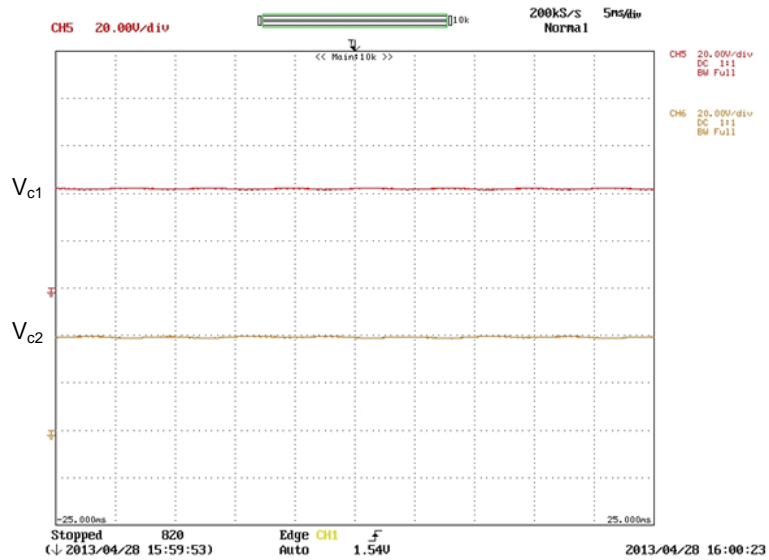


Figure 21. DC link capacitor voltages ( $V_{c1}$  and  $V_{c2}$ ) of NPC AFE 3-level converter under steady state condition

X axis: Time- 10ms/div, Y axis:  $V_{c1}$  and  $V_{c2}$  - 20 V/div

The transient response of the converter is evaluated with sudden change in load. The dc link voltages ( $V_{c1}$  and  $V_{c2}$ ) and line current of phase ‘a’ ( $i_{sa}$ ) has been observed when load is suddenly increased as shown in Figure.22. It can be clearly observed that the dc link voltages ( $V_{c1}$  and  $V_{c2}$ ) decreased when load is suddenly increased thereafter few cycles the dc link voltages recover to its desired voltage. The behaviour of the converter is also observed when load is reduced. The

dc link voltages suddenly increased and after few cycles it gets back to its desired value, shown in Figure.23. The response of the NPC AFE 3-level converter during transient found satisfactory with UPC, and confirmed that UPC is effectively able to regulate dc link voltage quickly at desired value during transient condition

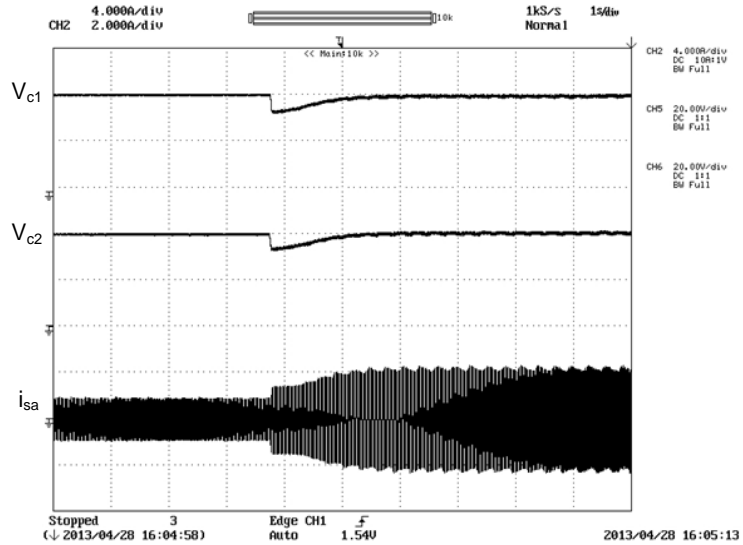


Figure 22. DC link capacitor voltages ( $V_{c1}$  and  $V_{c2}$ ) and line current ( $i_{sa}$ ) of NPC AFE 3-level converter when load is increased

X - axis: Time – 1s/div, Y - axis:  $V_{c1}$  and  $V_{c2}$  - 20 V/div,  $i_{sa}$  – 4 A/div

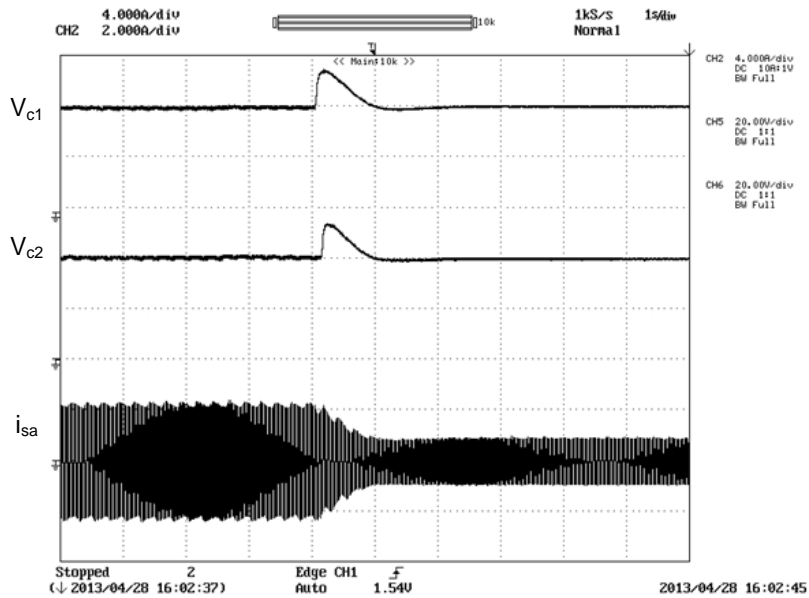


Figure.23 DC link capacitor voltages ( $V_{c1}$  and  $V_{c2}$ ) and line current ( $i_{sa}$ ) of NPC AFE 3-level converter when load is decreased

X - axis: Time – 1s/div, Y- axis:  $V_{c1}$  and  $V_{c2}$  - 20 V/div,  $i_{sa}$  – 4 A/div

### B.2 Neutral Point Potential (NPP) Control with NPP Regulator in UPC

It is experimentally verified that multilevel structures have inherent problem of NPP variation. Figure. 24 shows variation of NPP before and after the NPP regulator included in  $t = 3$  sec for  $\sigma = 33.33\%$ , which verifies the effective working of NPP regulator in UPC.

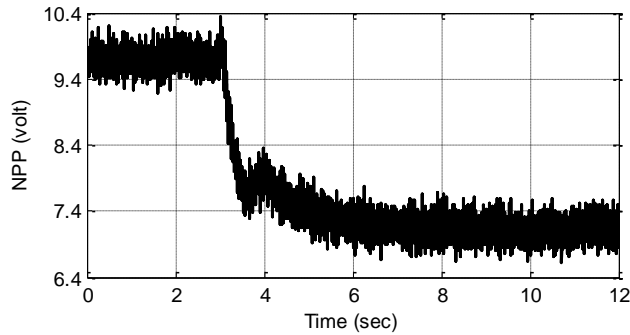


Figure 24. NPP variation before and after NPP regulator included in UPC at  $t = 3$  sec for  $\sigma = 33.33\%$  (Control Desk Layout)

### B.3 Neutral Point Potential (NPP) Control with Auxiliary Circuit

The function of auxiliary circuit has also been verified experimentally. Figure. 25 shows the dc link capacitor voltages ( $V_{c1}$  &  $V_{c2}$ ) before and after auxiliary circuit included in the system for  $\sigma = 33.33\%$ . As shown in the Figure. 25 the dc link capacitor voltages are not completely balanced because of series resistance  $r$  is connected with auxiliary capacitor  $C_a$  to limit the amplitude of the charging current for practical consideration. The presented result confirms the working of auxiliary circuit adopted to balance the dc link capacitors voltage.

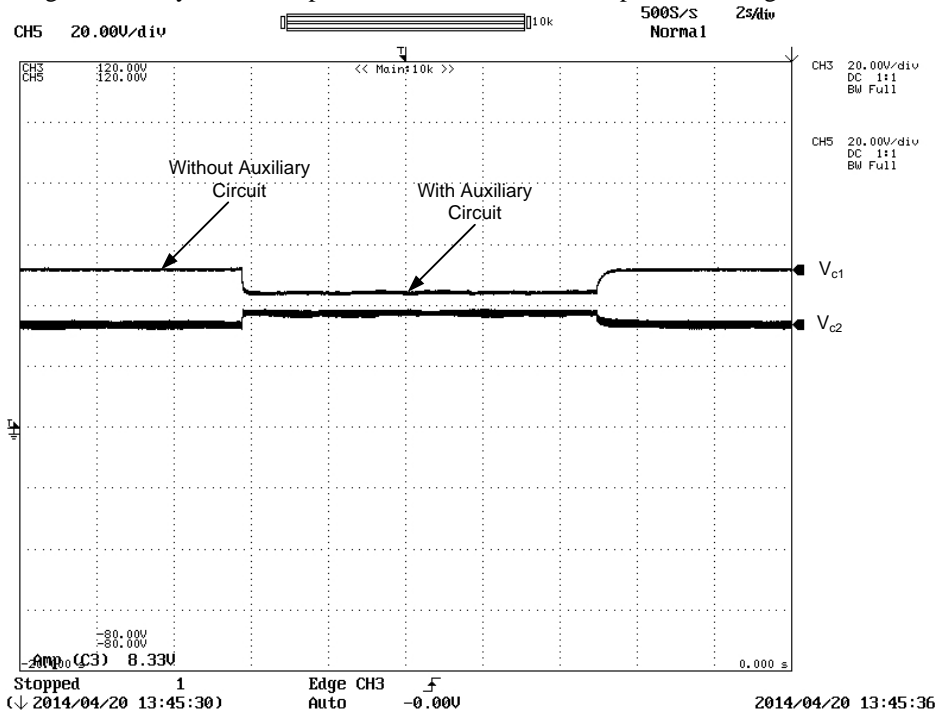


Figure 25. DC link capacitor voltages ( $V_{c1}$  and  $V_{c2}$ ) before and after auxiliary circuit included in the system for  $\sigma = 33.33\%$

X - axis: Time – 1s/div, Y- axis:  $V_{c1}$  and  $V_{c2}$  - 20 V/div

#### 4. Conclusion

The unity power factor controller (UPC) is presented to control NPC AFE 3-level converter for improved power quality at input and load side. The performance of three-phase NPC AFE 3-level converter has been evaluated with unity power factor controller. Simulation results are presented to study the performance of the system during transients as well as in steady state. It is observed that 3-level converter is operating at almost unity power factor with supply current THD within the limits imposed by IEEE519 standard. Simulated results also show that NPP regulator in conjunction with UPC is able to balance the capacitor voltages under balanced and unbalanced load with the addition of dc off-set in supply line current. The simulation results with an auxiliary circuit to balance the dc link capacitor voltages show effective balancing of dc link capacitor voltages without any adverse effects in terms of power quality. The features of UPC with NPP regulator and auxiliary circuit, observed in simulation study are also validated through experimentation performed on the low power prototype developed in laboratory using dSPACE DS 1103. Further, it can be concluded that the UPC with NPP regulator is suitable for drives application where depth of unbalance is not much whereas an auxiliary circuit is effective for active power filter where depth of unbalance is high.

#### 5. References

- [1]. Abdul Hamid Bhat, Pramod Agarwal, Three-phase, power quality improvement ac/dc converters, *Electric Power Systems Research*, Volume 78, Issue 2, pp 276-289, Feb 2008
- [2]. Rashid M. H., Power Electronics Handbook, Academic Press, New York, 2001.
- [3]. Sen P. C., Power Electronics, Tata McGraw Hill Pub., 1998.
- [4]. Akagi, H. , New Trends in Active Filters for Power Conditioning, Industry Applications, *IEEE Transactions on* , vol.32, no.6, pp.1312-1322, Nov/Dec 1996.
- [5]. El-Habrouk, M.; Darwish, M.K.; Mehta, P., Active power filters: A Review,"*Electric Power Applications*, **IEE Proceedings**, vol.147, no.5, pp.403-413, Sep 2000.
- [6]. Jain, S.K.; Agrawal, P.; Gupta, H.O.;, Fuzzy logic controlled shunt active power filter for power quality improvement, *Electric Power Applications*, *IEE Proceedings*, vol.149, no.5, pp. 317- 328, Sep 2002.
- [7]. Yang, S.P.; Chen, S.J.; Lin, J.L., Dynamics analysis of a low-voltage stress single-stage high-power factor correction ac/dc flyback converter, *Power Electronics*, *IET*, vol.5, no.9, pp.1624,1633, November 2012
- [8]. Lin Chengwu; Ba Dong, Research on AFE Technology in Multi-inverter System, Measuring Technology and Mechatronics Automation (ICMTMA), 2013 *Fifth International Conference on*, vol., no., pp.875,878, 16-17 Jan. 2013
- [9]. Xiaofeng Yang; Zheng, T.Q.; Zhiqin Lin; Tao Xiong; Xiaojie You, Power quality controller based on hybrid modular multilevel converter, Industrial Electronics (ISIE), 2012 *IEEE International Symposium on* , vol., no., pp.1997,2002, 28-31 May 2012
- [10]. Marchesoni M. and Tenca P., Diode-clamped multilevel converters: A practicable way to balance dc-link voltages," *IEEE Trans. on Industrial Electronics*, vol. 49, no. 4, August 2002.
- [11]. Midavaine H., Moigne P. L., and Bartholomeus P., "Multilevel three-phase rectifier with sinusoidal input currents, in Proc. *IEEE PESC'96*, 1996, pp. 1595-1599.
- [12]. Ridriguez J. Rodriguez D., Silva C., and Wiechmann E., A simple Neutral Point Control for Three-Level PWM Rectifiers, *European Power Electronics Conference*, EPE'99, 1999, pp. 1-8.
- [13]. J S Lai and F Z Peng. Multilevel Converters: A New Breed of Power Converters, *IEEE Transactions on Industry Applications*, vol 32, no 3, May/June 1996, pp 509-517.

- [14]. Fanuelo, L.G.; Rodriguez, J.; Leon, J.I.; Kouro, S.; Portillo, R.; Prats, M.A.M.; , The age of multilevel converters arrives, *Industrial Electronics Magazine, IEEE*, vol.2, no.2, pp.28-39, June 2008
- [15]. Krishna Kumar Gupta, Shailendra Jain, A Multilevel Voltage Source Inverter (VSI) to maximize the number of levels in output waveform, *International Journal of Electrical Power & Energy Systems*, Volume 44, Issue 1, January 2013, Pages 25-36.
- [16]. Ojha, Amit; Chaturvedi, P.K.; Mittal, Arvind; Jain, S., Carrier Based Common Mode Voltage Reduction Techniques in Neutral Point Clamped Inverter Based AC-DC-AC Drive System, *Journal of Power Electronics*, Vol. 16, Issue 1, pp 142-152, Jan. 2016
- [17]. Karuppusamy, P.; Vijayakumar, G.; Sathishkumar, S., Certain Investigation on Multilevel Inverters for Photovoltaic Grid Connected System, *Journal of Circuits, Systems and Computers*, doi:10.1142/S0218126616501085
- [18]. Bhat, A.H.; Agarwal, P., An Improved Performance Three-Phase Neutral-Point Clamped Rectifier with Simplified Control Scheme, *Industrial Electronics, 2006 IEEE International Symposium on*, vol.2, no., pp.1019-1024, 9-13 July 2006
- [19]. Kanaan, H.Y.; Al-Haddad, K.; Fnaiech, F., DC load unbalance and mains disturbances effects on a three-phase three-switch three-level boost rectifier, *Industrial Electronics, 2003. ISIE '03. 2003 IEEE International Symposium on*, vol.2, no., pp. 1043- 1048 vol. 2, 9-11 June 2003
- [20]. Shu, Z.; He, X.; Wang, Z.; Qiu, D.; Jing, Y.; , Voltage Balancing Approaches for Diode-Clamped Multilevel Converters Using Auxiliary Capacitor-Based Circuits, *Power Electronics, IEEE Transactions on* , vol.28, no.5, pp.2111-2124, May 2013
- [21]. Pou Josep, Boroyevich Dushan, and Pindado Rafael, New Feed forward Space-Vector PWM Method to Obtain Balanced AC Output Voltage in a Three-Level Neutral-Point-Clamped Converter, *IEEE Trans. on Industrial Electronics*, Vol. 49, No. 5, Oct. 2002, pp.1026-1034.
- [22]. Ojo Olorunfemi, and Konduru Srikanth, A Discontinuous Carrier Based PWM Modulation Method for the Control of Neutral Point Voltage of Three-Phase Three-Level Diode Clamped Converters, *Proc. PESC 2005*, Vol. 1, pp. 1652-1658.
- [23]. Li Jun, Huang Alex Q. Qian Zhaoming, and Zhao Huijie, A Novel Carrier Based PWM Method for 3-Level NPC Inverter Utilizing Control Freedom Degree, *Proc. of NPSC 2007*, pp. 1899-1904.
- [24]. Ishida, T.; Matsuse, K.; Sugita, K.; Lipei Huang; Sasagawa, K., DC voltage control strategy for a five-level converter, *Power Electronics, IEEE Transactions on*, vol.15, no.3, pp.508-515, May 2000
- [25]. Kouro, S.; Malinowski, M.; Gopakumar, K.; Pou, J.; Franquelo, L.G.; Bin Wu; Rodriguez, J.; Pérez, M.A.; Leon, J.I.; , Recent Advances and Industrial Applications of Multilevel Converters, *Industrial Electronics, IEEE Transactions on*, vol.57, no.8, pp.2553-2580, Aug. 2010
- [26]. Sano Kenichiro, and Fujita Hideaki, Voltage Balancing Circuit Based on a Resonant Switched Capacitor Converter for Multilevel Inverters, *IEEE Trans. on Industrial Electronics*, Vol. 44, No. 6, Nov/Dec. 2008, pp. 1768-1776.
- [27]. Chaturvedi, P.K.; Jain, S.; Agarwal, P.; Reduced switching loss pulse width modulation technique for three-level diode clamped inverter, *Power Electronics, IET*, vol.4, no.4, pp.393-399, April 2011
- [28]. Chaturvedi PK, Jain S, Agrawal P, Nema RK, Sao KK., Switching losses and harmonic investigations in multilevel inverters, *IETE Journal of Research*, Vol. 54, Issue 4, pp. 297-307, Jul/Aug 2008,
- [29]. Shu, Z.; He, X.; Wang, Z.; Qiu, D.; Jing, Y.;, Voltage Balancing Approaches for Diode-Clamped Multilevel Converters Using Auxiliary Capacitor-Based Circuits, *Power Electronics, IEEE Transactions on* , vol.28, no.5, pp.2111-2124, May 2013

- [30]. P. Chaturvedi, A. Ojha, S. Jain and A. Mittal, Unity power factor controller for neutral point clamped active front end converter with DC voltage balancing, 2016 *IEEE International Conference on Industrial Technology (ICIT)*, Taipei, Taiwan, 2016, pp. 384-389.



**Amit Ojha** was born in India, in 1974. He received B.E degree in Electrical Engineering from MACT, Bhopal, India, in 1998. He received M. Tech. and Ph. D. degrees from Maulana Azad National Institute of Technology (MANIT), Bhopal, India, in 2002 and 2013, respectively. He studied multilevel converter fed induction motor drives while working towards his Ph. D. He has had more than 15 years of teaching experience and more than 5 years of research experience. He is presently working as an Assistant Professor in Department of Electrical Engineering, MANIT. His current research interests include electrical machines, power electronics, electric drives, high-power-factor converters, and multilevel converters.



**Pradyumn Chaturvedi** received B.E. degree in Electrical Engineering from Barkatullah University, Bhopal, India, in 1996; M.E. degree in Power Electronics from the Rajiv Gandhi Technical University, Bhopal, India, in 2001; and Ph.D. degree from the National Institute of Technology, Bhopal, India, in 2010. He has had 14 years of teaching experience. He is presently working as an Assistant Professor in the Department of Electrical Engineering, NIT, Nagpur, India. He has published more than 45 research papers in referenced national and international journals and conferences. His current research interests include electrical drives, high-power-factor converters, photovoltaic power conditioning systems, and multilevel inverters.



**Arvind Mitral** obtained B.E. degree in Electrical Engineering from Maulana Azad National Institute of Technology (MANIT), Bhopal, India, in 1991, securing first position in the university (Gold Medallist). He is a post graduated in Power Apparatus and Electrical Drives (PAED) at the Indian Institute of Technology Roorkee, Roorkee, India, in 1993, and obtained Ph.D. degree from Barkatullah University, Bhopal India, in 2002. He is presently an Associate Professor in the Energy Centre, MANIT, Bhopal, India. He has had more than 23 years of experience in teaching undergraduate and postgraduate students. He is a life member of the ISTE and an Associate Member of the Institution of Engineers. He has guided two Ph.D. candidates and published several papers in various national and international conferences and journals. He has also authored seven engineering books.



**Shailendra Jain** received B.E. degree in Electrical Engineering from Samrat Ashok Technological Institute (SATI), Vidisha, India, in 1990; M.E. degree in Power Electronics from the Shri Govindram Seksaria Institute of Technology and Science, Indore, India, in 1994; Ph.D. degree from the Indian Institute of Technology, Roorkee, India, in 2003; and Post-Doctoral Fellowship from the University of Western Ontario, London, ON, Canada, in 2007. He is presently a Professor in the Department of Electrical Engineering, National Institute of Technology, Bhopal, India. His current research interests include power electronics and electric drives, power quality improvement, active power filters, high-power-factor converters, and fuel-cell-based distributed generation. Dr. Jain was a recipient of the “Career Award for Young Teachers” from the All India Council for Technical Education (AICTE), New Delhi, India, for the year 2003–2004.